

Temporal aspects of reflection and  
focusing of attosecond pulses

Master Thesis  
by  
Ola Synnergren

September 8, 2000  
LRAP-260

## **Abstract**

Attosecond laser pulses can be generated using harmonics. The temporal aspects of reflecting and focusing these pulses have been studied with a set of MATLAB programs designed for this. It is shown that mirrors destroy the pulse in some cases and work fine in other cases. Calculations on focusing pulses using curved mirrors and zone plates show that spherical mirrors are able to preserve the temporal pulse shape, while zone plates only are usable with single harmonics, not attosecond pulse trains. The calculations also show that the efficiency of the spherical mirrors is very low in normal incidence. The use of multilayer and elliptical mirrors are briefly discussed.

# Contents

<b>1</b>	<b>Introduction</b>	<b>4</b>
1.1	Femtosecond lasers . . . . .	4
1.2	Sub-femtosecond pulses . . . . .	4
1.3	Pulse length and line width . . . . .	5
1.4	Measuring short pulses . . . . .	6
1.5	Focusing optics . . . . .	7
1.6	Aberrations . . . . .	8
1.6.1	Spherical aberration . . . . .	8
1.6.2	Chromatic aberration . . . . .	8
1.7	Outline . . . . .	9
<b>2</b>	<b>Reflectivity and phase shift</b>	<b>10</b>
2.1	Introduction . . . . .	10
2.2	The Fresnel Equations . . . . .	10
2.3	Complex index of refraction . . . . .	11
2.4	Reflectivity and phase shift . . . . .	11
2.5	Calculations . . . . .	12
2.6	Results . . . . .	12
2.7	Conclusions . . . . .	13

<b>3</b>	<b>Reflection on plane surfaces</b>	<b>20</b>
3.1	Introduction . . . . .	20
3.2	Calculations . . . . .	20
3.3	Results . . . . .	21
3.4	Conclusions . . . . .	22
<b>4</b>	<b>Reflection on curved surfaces</b>	<b>27</b>
4.1	Introduction . . . . .	27
4.2	Calculations . . . . .	27
4.3	Results . . . . .	28
4.4	Conclusions . . . . .	28
<b>5</b>	<b>Diffractive XUV optics</b>	<b>33</b>
5.1	Introduction . . . . .	33
5.2	Calculations . . . . .	33
5.3	Results . . . . .	34
5.4	Conclusions . . . . .	35
<b>6</b>	<b>Conclusions and perspectives</b>	<b>37</b>
<b>A</b>	<b>Program listings</b>	<b>40</b>
A.1	Reflection coefficients . . . . .	40
A.2	3D plot reflectivity and phase shift . . . . .	40
A.3	Reflection on plane surface . . . . .	41
A.4	Reflection on curved surface . . . . .	44
A.5	Focusing with zone plate . . . . .	46

# Chapter 1

## Introduction

### 1.1 Femtosecond lasers

The laser technology has developed a lot since the first laser was built. The maximum pulse energy and peak power have increased, while the minimum pulse duration has decreased (see reference [1]). By using broadband crystals and mode locking, laser pulses with duration down to five femtoseconds have become possible. These laser pulses are in the near infrared spectral region, where the duration of a single oscillation of the light is about 2.5 fs. Thus, the laser pulse only lasts a few cycles. It is not possible to decrease the pulse length much more as long as the laser pulses are generated in this spectral region. To generate shorter pulses, one has to use lasers with considerably shorter wavelengths. However, there are no lasers (except from some X-ray lasers) in this spectral region.

### 1.2 Sub-femtosecond pulses

One way of generating sub-femtosecond pulses might be to use the harmonics of a laser. If the light from a high power femtosecond laser is focused into a gas jet, high order harmonics can be obtained. These are not really laser pulses, but they have a very high degree of coherence. The high intensity in the gas gives rise to non-linear processes (see references [2] and [3]). Due to symmetry, only odd orders can be obtained. To get an attosecond pulse, the different harmonics need to be in phase. There are indications that this is possible if special precautions are taken.

To get a nice attosecond pulse, some of the harmonics are selected, preferably

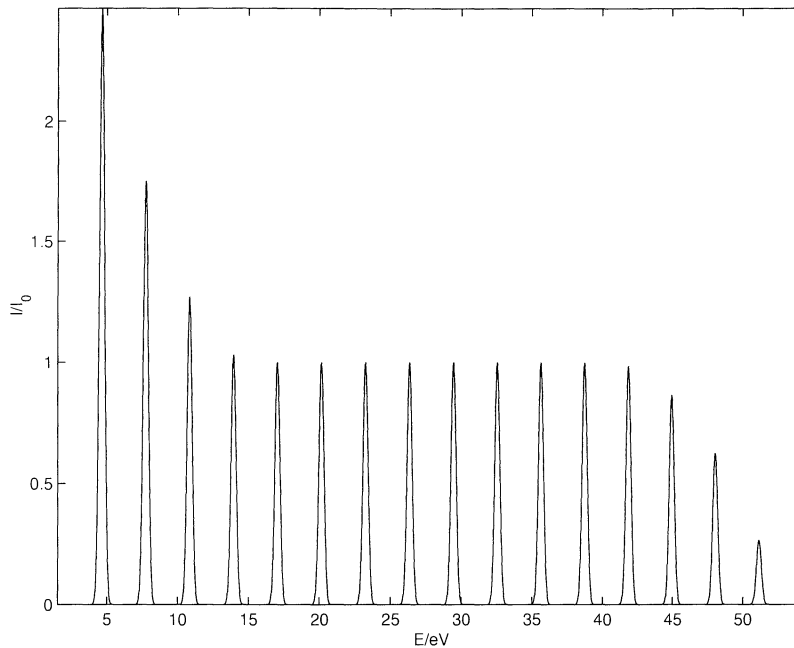


Figure 1.1: Schematic harmonic spectrum generated from a 10 fs 800 nm laser.

those from the plateau in Figure 1.1. They may be filtered out using a thin aluminum foil. If the 9th to the 21st harmonic is selected, the energy width would be approximately 18 eV and the pulse duration would be a few hundred attoseconds (see reference [4]).

Dealing with these pulses requires a great deal of care. There is no known material that does not absorb light in the extreme ultraviolet (XUV) region. Hence, the attosecond pulses must always be handled in vacuum. Further problems occur when the pulse is reflected or focused. Since all materials are absorbing in the wavelength region of interest, phase shifts that alter the temporal pulse shape may be introduced.

### 1.3 Pulse length and line width

As mentioned earlier, one must have a broad spectrum to obtain a short pulse. The relationship between the duration of a pulse,  $\Delta t$ , and the spectral line width,  $\Delta\nu$ , is

$$\Delta t \Delta \nu \geq 1 \quad (1.1)$$

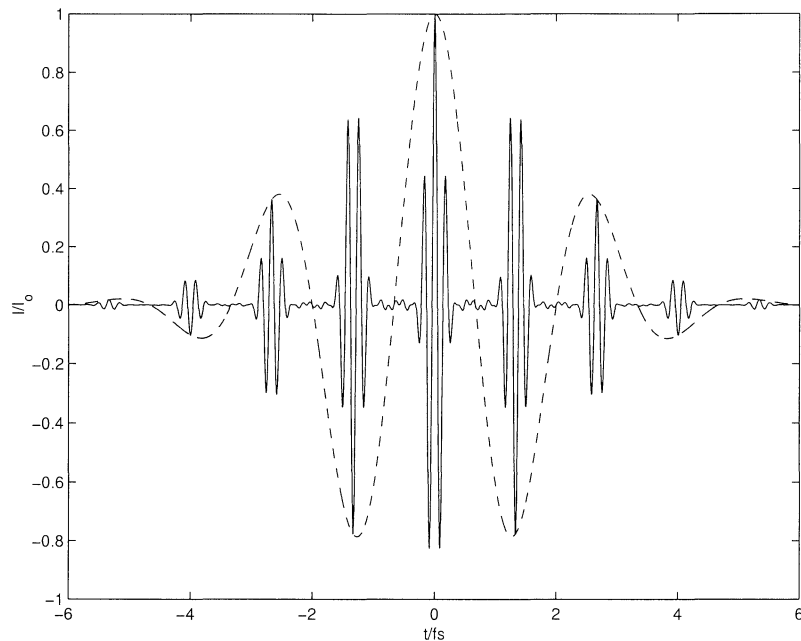


Figure 1.2: Comparison of the electric fields between a 5 fs short infrared laser pulse (dashed line), and a attosecond pulse generated with the 9th to the 21st harmonic of the infrared pulse (solid line).

In a Fourier limited pulse all frequencies are in phase and the product above has its minimum value (which depends on the pulse shape). The temporal pulse shape, as well as the shape of the spectrum, is typically Gaussian. Fourier limited pulses are very hard to achieve in reality. As soon as the pulse travels through an optical medium, the phase between the different frequencies is disturbed. The reason is that the medium has some dispersion, which means that the index of refraction depends on the wavelength.

## 1.4 Measuring short pulses

The diodes that exist today are not fast enough even to measure a femtosecond pulse. Autocorrelation is often used to measure the pulse duration of femtosecond pulses. The idea is to use the pulse itself for the measurement. A typical autocorrelator is a Michelson interferometer, with the movable mirror mounted on a piezoelectric crystal. The pulse is recombined, but with a small delay between the parts of the pulse that have been reflected at the different mirrors. Hence, the autocorrelation of the pulse can be measured.

The measurement goes from measuring extremely short times to measuring short distances (the translation of the mirror).

Today, we believe that attosecond pulses are created, but to be sure, measurements have to be done. Perhaps an autocorrelator can be used. There is a need for attosecond XUV optical components to do this, and the optical components should not alter the pulse. A lot of work has been done on XUV optics, for example by physicists using synchrotrons. However, these studies only deal with the spatial aspects of the problem, since there is no need for good temporal characteristics. For use with attosecond pulses, the temporal characteristics are at least as important as the spatial.

## 1.5 Focusing optics

All optical components are based on interference. The optical path length from the source to the focal point should be the same (or differ by an integer number of wavelengths) for every possible path from the source to the focal point, which will make the interference constructive. Optical components based on equal path lengths are lenses and mirrors. The lenses are made out of a material that have a larger index of refraction than the surrounding medium. The beams that are going straight from the source to the focal point are passing through the thick part of the mirror, while the beams that are not going in a straight line are passing the mirror in a thinner part. This makes the *optical* path length equal.

Curved mirrors are also used as focusing optics. The curvature of the mirror makes the path length equal for all beams reflected by the mirror. It can be shown that the solution to this problem in the general case is elliptical mirrors. In some cases, the mirrors can have more simple forms. If the light source to be focused is very distant, the mirrors become parabolic, as known from the parabolic antennas used to receive television broadcasts from satellites. If the object point and image point is the same, the ellipse becomes a sphere, and a spherical mirror can be used to focus the light. In many cases, however, spherical mirrors are good enough to focus light even if there is a small distance between the object and the image. This will be discussed further in section 1.6.

It is also possible to make focusing optics where the path lengths differ by an integer number of wavelengths, since this also will make the interference constructive at the focal point. The Fresnel lenses (commonly used in OH projectors) are based on this. These lenses are normal lenses, made almost flat by removing some of the mirror material. The drawback is that the chromatic aberration becomes much worse. The reason is that the path



length should differ by an integer number of wavelengths.

The Fresnel zone plate is another kind of focusing optics (see reference [5]). It consists of a number of dark and bright areas. These areas are arranged so that the light that is in phase at the focal point passes through the bright areas, while the light that would arrive out of phase is removed by the dark areas. This kind of optics is mostly used for x-rays, where there are no materials suitable for mirrors and lenses. The efficiency of the zone plates can be improved by replacing the dark areas with some phase retarding material, so that the phase is turned half a period, and all light arrives in phase at the focal point. The zone plates have a large chromatic aberration.

## 1.6 Aberrations

### 1.6.1 Spherical aberration

Since spherical lenses and mirrors are easier to fabricate than parabolic and elliptical mirrors, they are widely used. However, the more the beam differs from the assumptions in the paraxial approximation, the bigger the aberration becomes. For on-axis spherical mirrors and lenses, the biggest aberration is the spherical aberration. This means that the beams that passes through/is reflected in the outer parts of the lens/mirror has a different focal length than the beams in the center of the optics.

For normal light, the spot size and shape are the only things that have to be considered when there are aberrations. For extremely short pulses, one has to remember that the aberrations also stretch the pulse in time. The reason is that the optical path lengths are not equal. The portion of the pulse that is focused by one part of the optics with a larger optical path length arrives later at the focal point.

### 1.6.2 Chromatic aberration

As mentioned earlier, lenses are made out of a material that has a higher index of refraction than the surrounding medium. The shape of the lens and the index of refraction determines the focal length of the lens. Since the material has dispersion (the index of refraction is dependent on the wavelength), the focal length is also dependent on the wavelength. This is called *chromatic aberration*.

Normally, mirrors have no chromatic aberration, since the phase shift on the mirror does not depend on the wavelength. For absorbing materials,

however, there is a phase shift dependent on the wavelength. Since most materials are absorbing in the XUV region, mirrors for reflecting attosecond pulses may suffer of chromatic aberration. This will be discussed in Chapter 2.

## 1.7 Outline

As mentioned earlier, this report focuses on the temporal aspects of attosecond optical components. The aim with the project was to create a set of MATLAB programs that can be used to calculate what is happening with the pulse at various optical components. When used together, they are supposed to be able to do calculations on optical setups. The programs have been used to study some specific cases.

Chapter 2 deals with reflectivity and phase shift, and the aim is to identify problems that may occur in optical systems.

In Chapter 3 the effect of reflection on a plane surface is studied. Plane mirrors are used in most optical systems to transfer the pulse between different optical components.

Focusing mirrors are studied in Chapter 4. The aim is to see the effects of using a spherical mirror to focus the attosecond pulse.

Finally, zone plates are studied in Chapter 5. The differences from focusing mirrors are examined.

## Chapter 2

# Reflectivity and phase shift

### 2.1 Introduction

When light hits a surface, a certain part of the light is reflected, and the other part is transmitted (see Figure 2.1). There might also be a phase shift when the light is reflected or transmitted. This only occurs in certain intervals of incidence angle for non-absorbing materials. For absorbing materials, however, there is a phase shift for most angles, see section 2.2. Since most materials are absorbing in the region of interest for attosecond optics, this has to be taken into consideration.

### 2.2 The Fresnel Equations

It can be shown that the amplitude reflection and transmission coefficients can be written (see reference [6] and [7])

$$r_p = \frac{n_t \cos \theta_i - n_i \cos \theta_t}{n_t \cos \theta_i + n_i \cos \theta_t} \quad (2.1)$$

$$r_s = \frac{n_i \cos \theta_i - n_t \cos \theta_t}{n_i \cos \theta_i + n_t \cos \theta_t} \quad (2.2)$$

$$t_p = \frac{2n_i \cos \theta_i}{n_i \cos \theta_t + n_t \cos \theta_i} \quad (2.3)$$

$$t_s = \frac{2n_i \cos \theta_i}{n_i \cos \theta_i + n_t \cos \theta_t} \quad (2.4)$$

with denotations according to Figure 2.1.

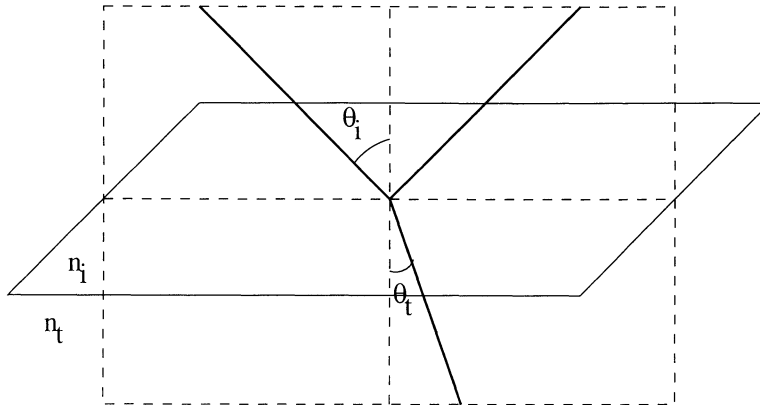


Figure 2.1: Reflection and transmission of beam.

### 2.3 Complex index of refraction

The above equations are valid for materials with no absorption. If the material has absorption, it can be shown that the above relations apply if the complex index of refraction is used. The complex index of refraction can be written as (see reference [8])

$$n = n_R + i\mu \frac{\lambda}{4\pi} \quad (2.5)$$

where  $n_R$  is the real index of refraction, and  $\mu$  is the absorption coefficient. For use with X-rays, the complex index of refraction is often written [10]

$$n = 1 - \delta + i\beta \quad (2.6)$$

and  $\delta$  and  $\beta$  are tabulated. The fact that there is a negative sign in front of  $\delta$  indicates that the real part often is below 1, which means that the phase velocity is greater than the speed of light.

### 2.4 Reflectivity and phase shift

The reflectivity  $R$  is the fraction of energy that is reflected on the surface. It may be written as

$$R = rr^* \quad (2.7)$$

The phase shift of the electric field is the same as the phase angle of  $r$ .

## 2.5 Calculations

By using the Fresnel equations of reflection coefficients the reflectivity and phase shift were calculated for energies in the range 10 eV to 30 eV, and for angles of incidence from  $1^\circ$  to  $90^\circ$ . The calculations were done for three different materials: aluminum, gold and platinum. The indices of refraction used were taken from [9]. The MATLAB program used for the calculations can be found in Appendix A.

## 2.6 Results

The figures 2.2 to 2.7 show the calculated reflectivity and phase shift for different materials, energies and angles of incidence. As can be seen in these figures, the reflectivity and phase shift are strongly dependent on the photon energy and the angle of incidence. There is a big difference between the different materials. For example, the reflectivity and phase shift for reflection on gold is less dependent on the photon energy in the interval 10 eV to 30 eV than for reflection on aluminum.

Figure 2.2 shows the reflectivity on aluminum for p- and s-polarization. Aluminum has a band edge around 15 eV, which shows in the graph as a big drop in reflectivity. The Brewster angle can be found around  $30^\circ$  and 15 eV to 20 eV for the p-polarization. The reflectivity is (almost) zero in this area. A few other structures can be seen in the figures. Among these, there is a small increase in the reflectivity around 19 eV and 24 eV. This is probably due to the electron structure in aluminum.

The effect of the electron structure can also be seen in Figure 2.3. There is a small change in the phase shift for these energies. For near normal incidence, there is a plateau in the phase shift for photon energies above 15 eV. Due to the band edge mentioned above, the plateau ends at 15 eV.

The reflectivities for gold and platinum (Figure 2.4 and Figure 2.6) look very much like each other, but they look very different from the reflectivity of aluminum. A band edge effect, like the one at 15 eV for aluminum, is not present at all in these graphs. The Brewster angle can be seen in both figures, even more clearly than for aluminum. In both cases, the Brewster angle is larger than for aluminum, at about  $50^\circ$ . There are also traces of the electron structure in both cases. For gold, there are two peaks around 26 eV and 27 eV, and for platinum there is one peak at 29 eV.

These small peaks can also be seen in the phase shift (Figure 2.5 and Figure 2.7). Beside from this, the phase shifts of gold and platinum look very

similar to each other, but completely different from aluminum.

## 2.7 Conclusions

The reflectivity and phase shift are strongly dependent on the photon energy, angle of incidence and choice of material. When designing a mirror for XUV, one must consider which wavelength ranges that are of interest, and which angles that are possible to use. The material must then be chosen so that the reflectivity is high enough, while peaks in the reflectivity and phase shift should be avoided.

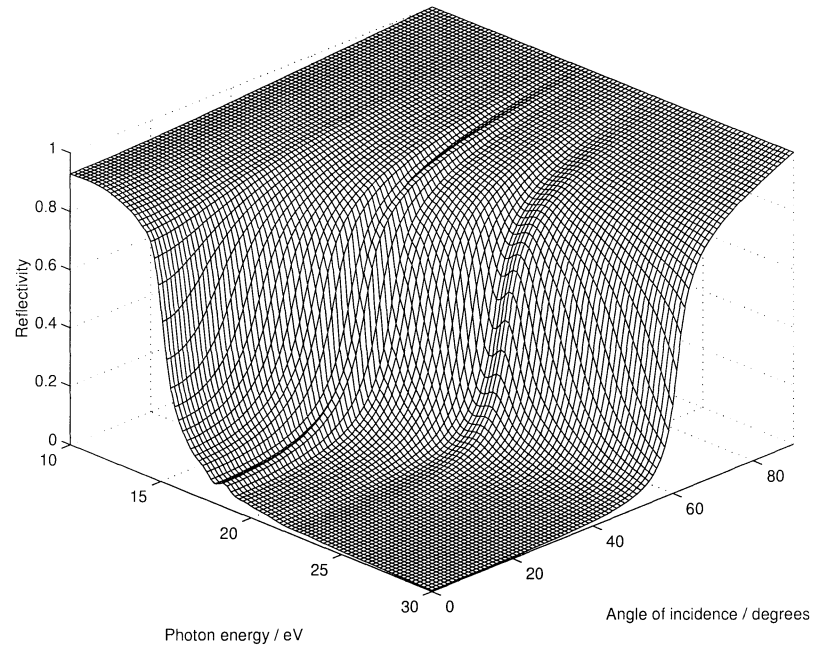
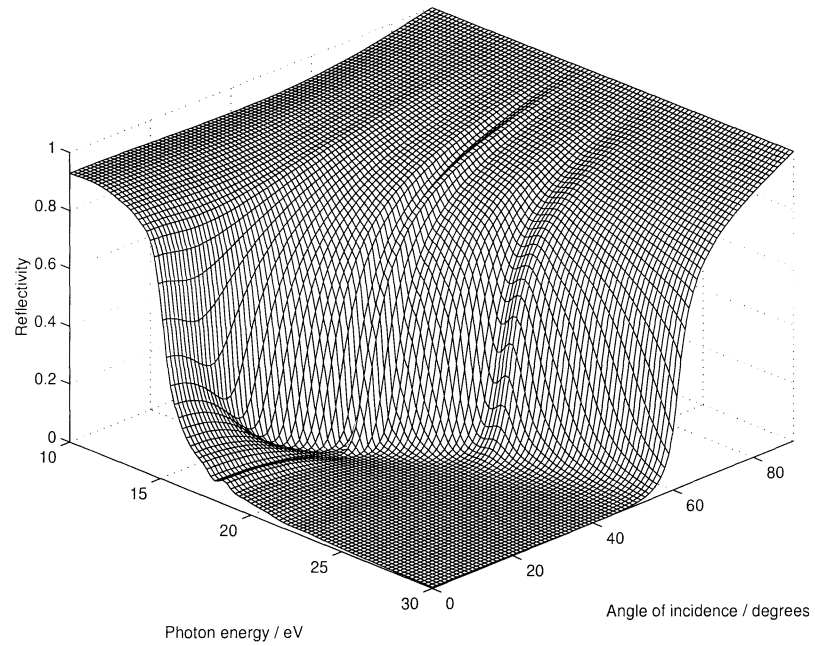


Figure 2.2: Reflectivity of aluminum as function of wavelength and angle of incidence. The upper figure is for p-polarization and the lower is for s-polarization. The Brewster angle can be seen in the upper figure, between 15 eV and 20 eV photon energy, and  $20^{\circ}$  and  $40^{\circ}$  incidence angle.

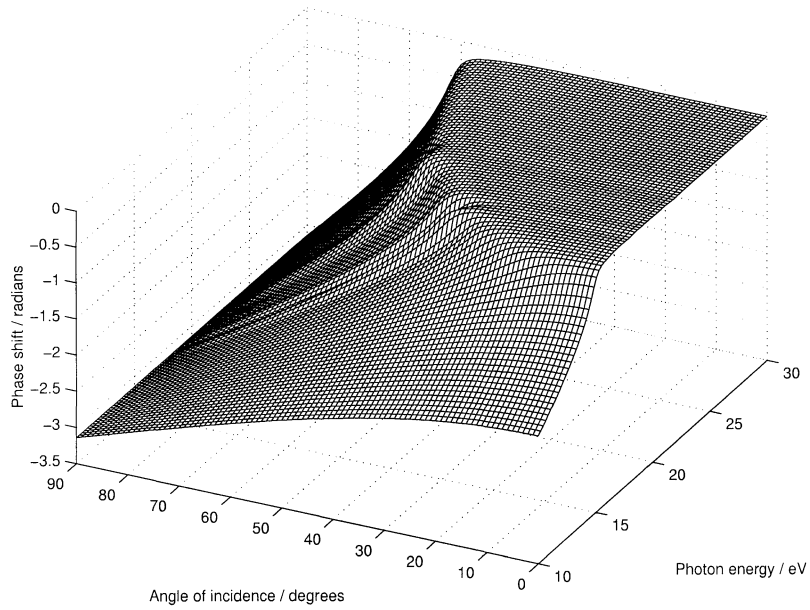
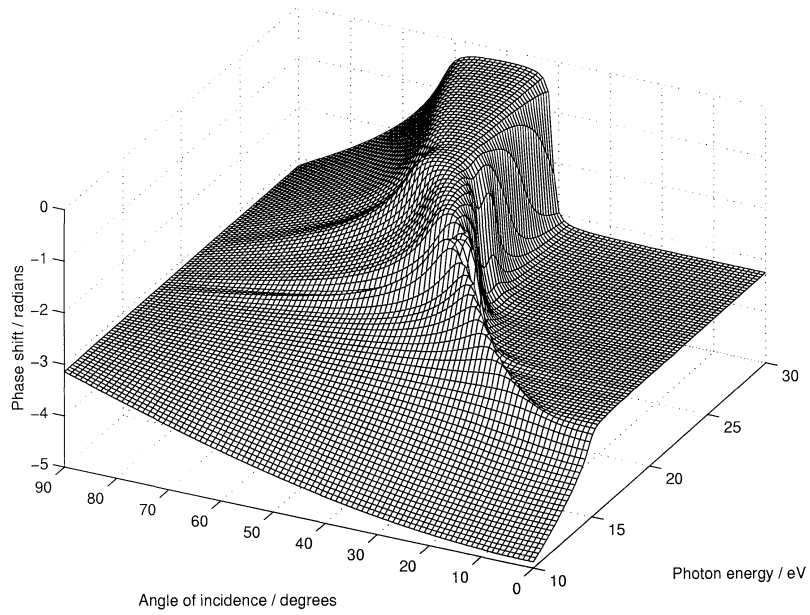


Figure 2.3: Phase shift of aluminum as function of wavelength and angle of incidence. The upper figure is for p-polarization and the lower is for s-polarization.



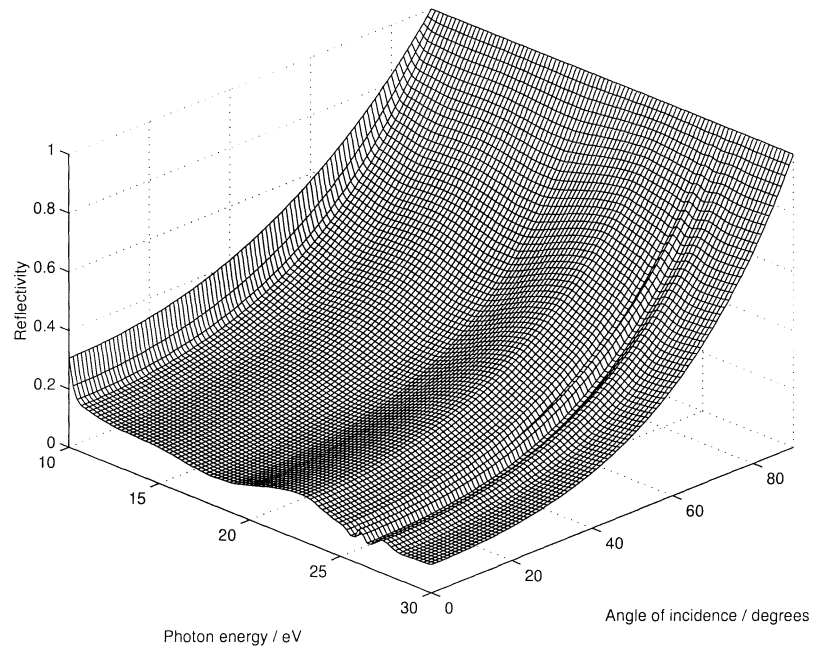
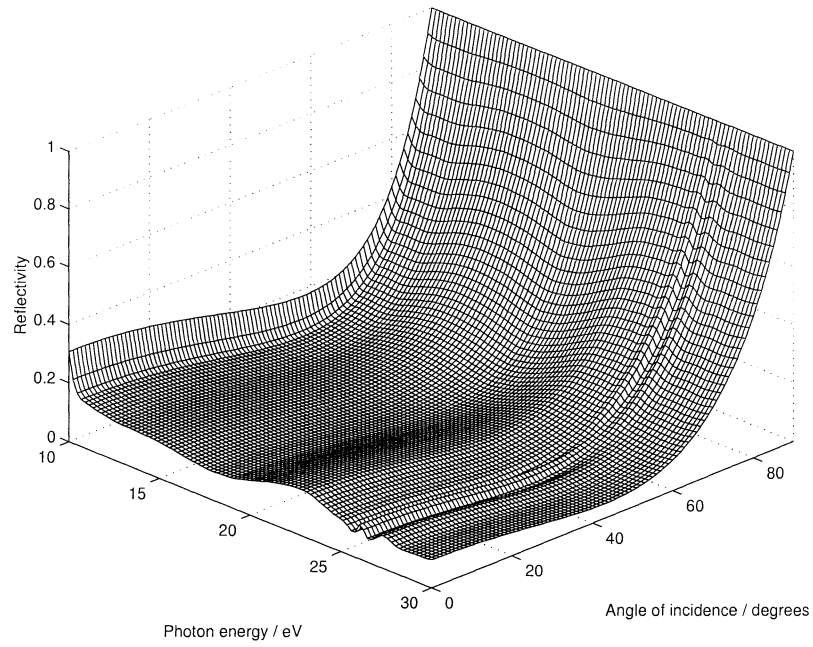


Figure 2.4: Reflectivity of gold as function of wavelength and angle of incidence. The upper figure is for p-polarization and the lower is for s-polarization.

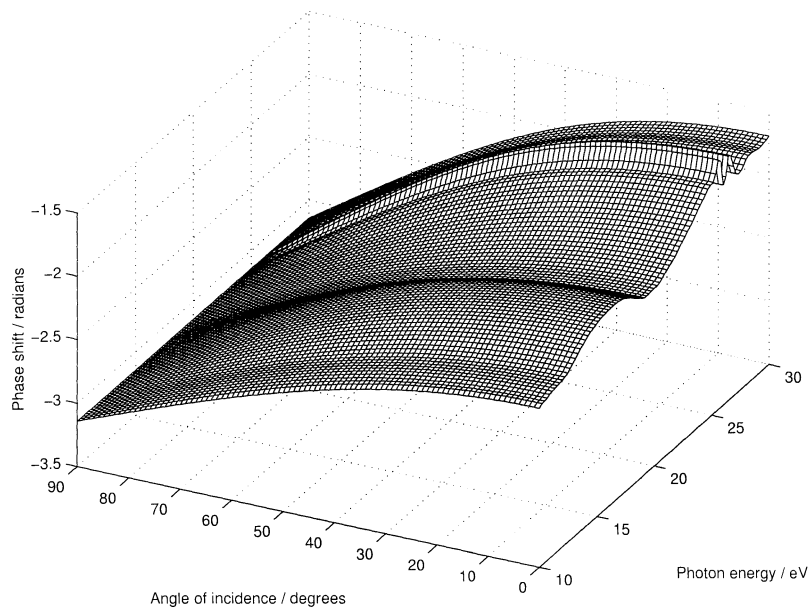
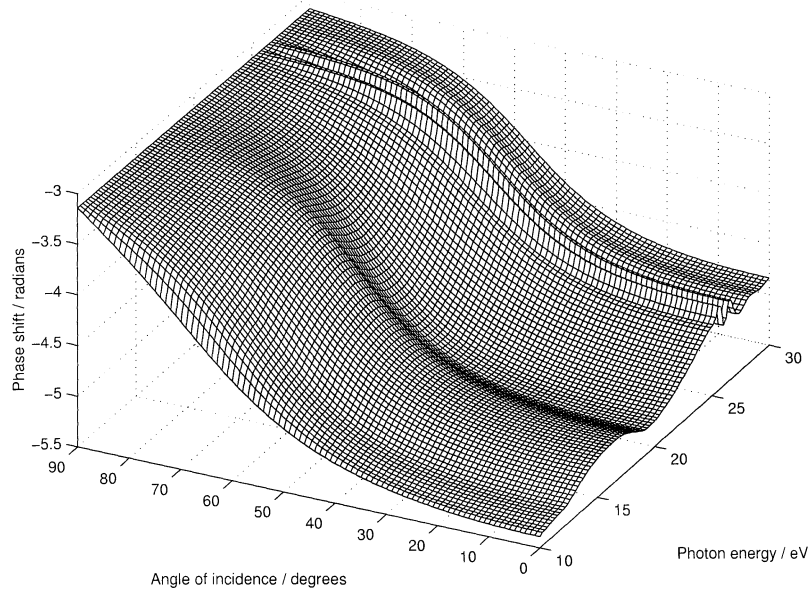


Figure 2.5: Phase shift of gold as function of wavelength and angle of incidence. The upper figure is for p-polarization and the lower is for s-polarization.

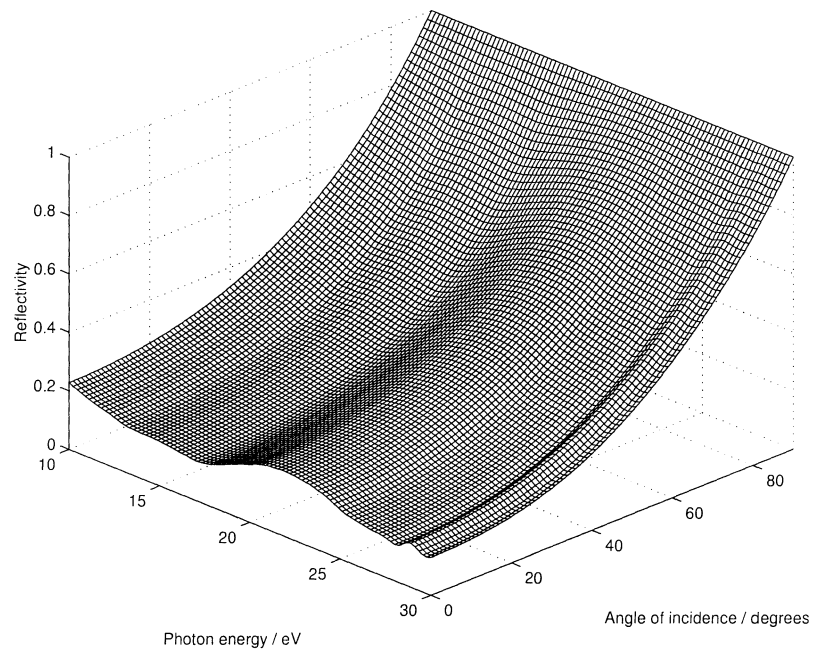
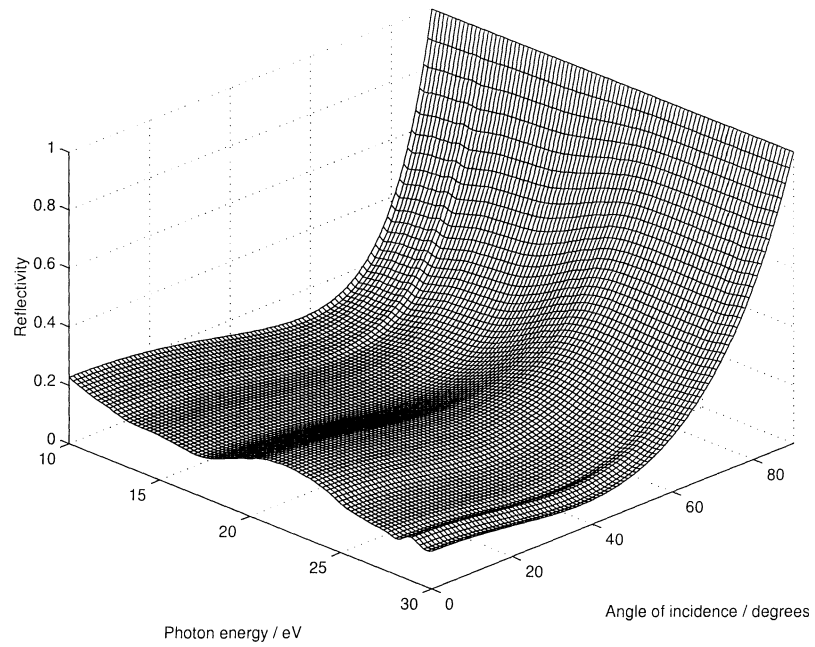


Figure 2.6: Reflectivity of platinum as function of wavelength and angle of incidence. The upper figure is for p-polarization and the lower is for s-polarization.

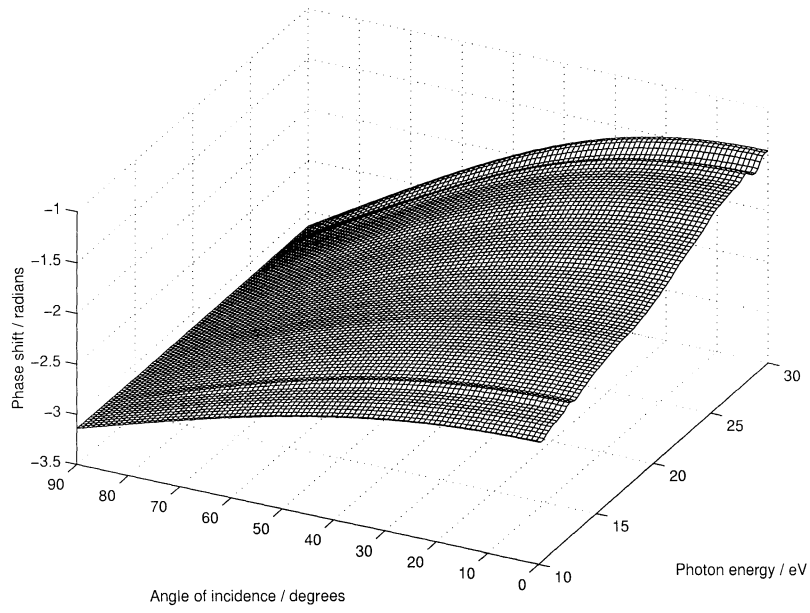
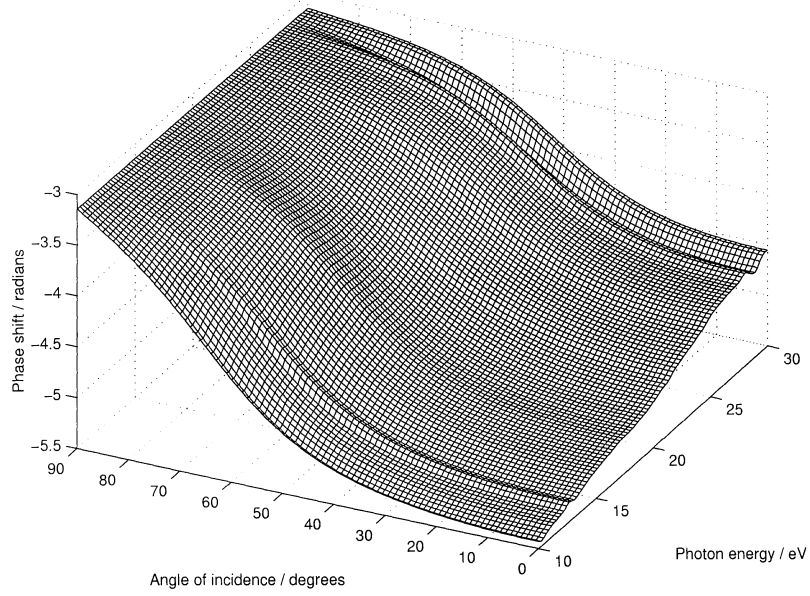


Figure 2.7: Phase shift of platinum as function of wavelength and angle of incidence. The upper figure is for p-polarization and the lower is for s-polarization.

## Chapter 3

# Reflection on plane surfaces

### 3.1 Introduction

An attosecond pulse has a very broad spectral bandwidth. The frequencies are phase locked, which gives a very short pulse length, as discussed in Chapter 1. When a pulse is reflected, the phase shift depends on the photon energy. This may disturb the phase locking, and if it does, it will alter the pulse shape. The pulse will become longer in time if it is transform limited from the beginning (which is assumed). In addition, the reflectivity is also dependent on the photon energy, which also contributes to the change in pulse shape.

### 3.2 Calculations

In order to investigate how a pulse is altered by a reflection on a plane surface, a MATLAB program was written. The assumptions used in the specific cases examined were

- Harmonics are generated from an 800 nm 10 fs laser.
- 9th to 21st harmonic are filtered out by a filter leaving all harmonics with equal intensity.
- Initially, all harmonics are in phase.
- Each harmonic has the same duration as the fundamental pulse (it is known that the harmonics shorter or as long as the fundamental pulse).

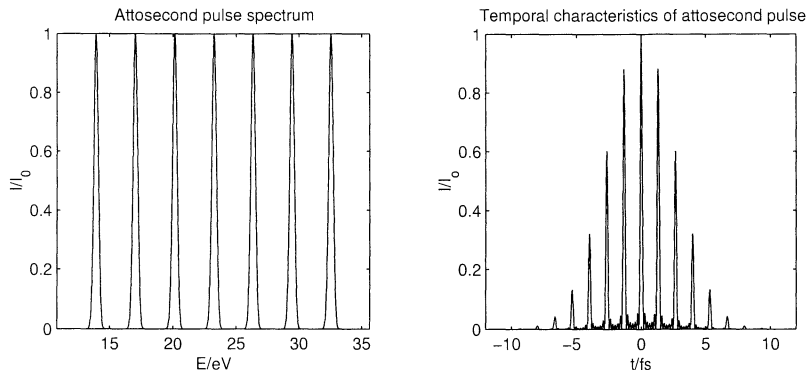


Figure 3.1: Pulse spectrum and temporal characteristics of attosecond pulse before reflection. The duration of a single attosecond pulse is 160 as (FWHM).

- The harmonics have no chirp from the beginning. This is actually not the case, but it is assumed for simplicity.

The indices of refraction needed for these calculations were taken from reference [9]. The program begun with creating a harmonic spectrum according to Figure 3.1. It then calculated the reflectivity coefficients as a function of energy, and used this to calculate the spectrum after reflection. The program used Fast Fourier Transforms (FFT) to calculate the temporal characteristics of the attosecond pulse train. The MATLAB program used for the calculations can be found in Appendix A.

### 3.3 Results

In order to examine the effects from the reflectivity and the phase shift, each plot shows the effect from the reflectivity alone, the phase shift alone, and the combined effect from both. The effects from a phase shift are shown in Figure 3.3. The reflectivity here differ very much between the different harmonics, except from the 21st. There is almost no effect from the reflectivity. However, the phase shift differs between the different harmonics, which delays the attosecond pulse about 90 as, and increases the background.

The effects from the decrease in reflectivity can be seen in Figure 3.4. The phase shift is constant here, though the reflectivity is much smaller for the larger photon energies. A small broadening of the pulse can be seen, but there is also an increase in background. The pulse duration increases from 200 as to 240 as.

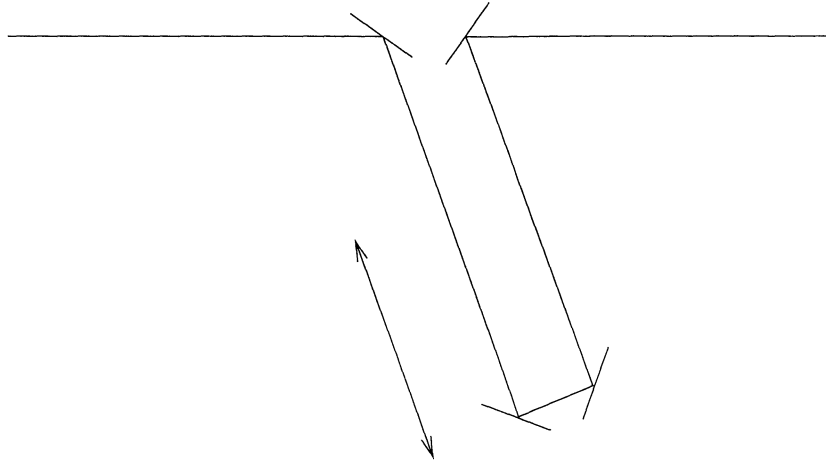


Figure 3.2: A delayline. The pulse is delayed by a time adjustable by moving the mirrors in the direction of the arrow.

In the cases mentioned above, there is only a contribution from the phase shift or the reflectivity. In many cases, there are effects from both. If this is the case, the result can be something completely different from the results from just one of the factors. An example can be seen in Figure 3.5. The duration of the pulse would now be 840 as instead of 160 as.

From the cases above (Figure 3.3 and 3.4), it may seem like it is no big problem to reflect attosecond pulses. However, these figures only show a single reflection. A simple delay line, with  $50^\circ$  angle to the original line may consist of two  $45^\circ$  mirrors, one  $25^\circ$  mirror and one  $65^\circ$  mirror (see Figure 3.2). The result from this system is shown in Figure 3.6. It can be seen that the pulse is no longer an attosecond pulse train.

### 3.4 Conclusions

When creating an optical system for the XUV region, it is important to consider what happens when a mirror is put into the beam. The number of reflections should be kept to a minimum. If it is possible, grazing incidence is the best choice. If it is not possible, for example in a delay line, it is very important to use the correct material and angle.

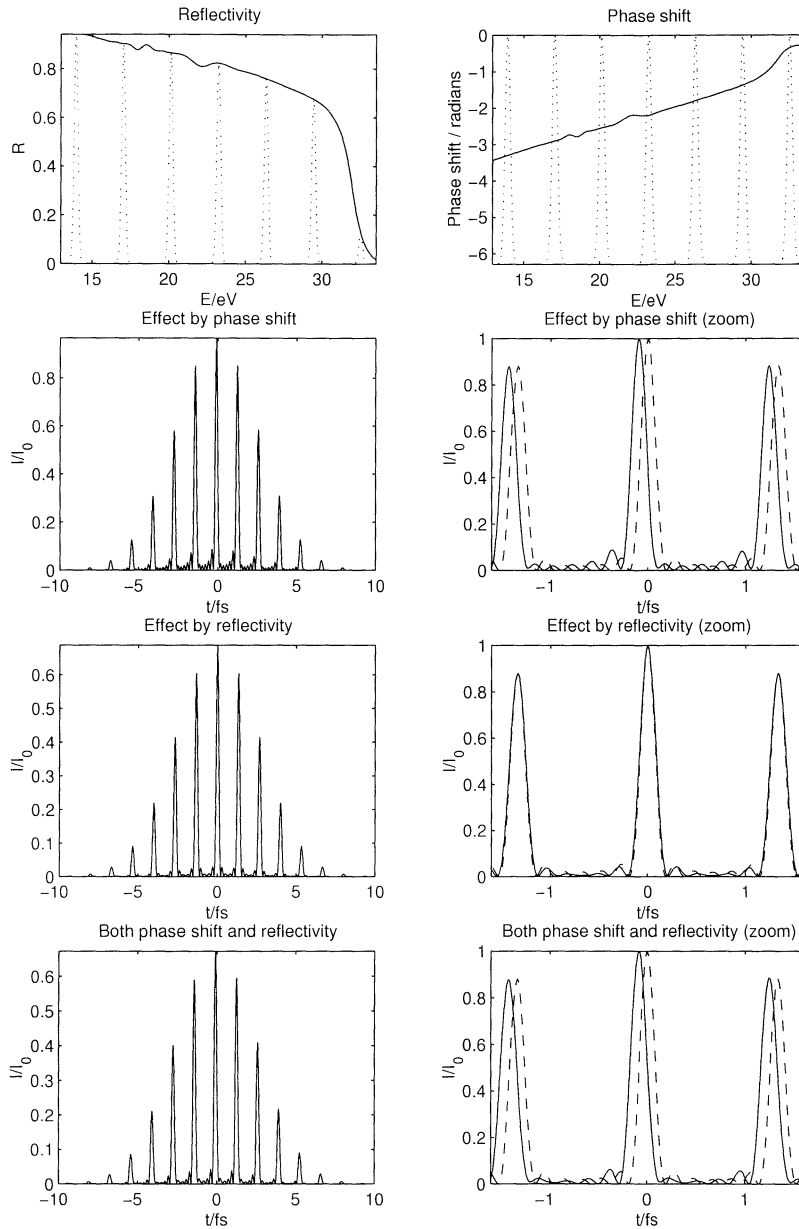


Figure 3.3: Pulse change at a reflection on aluminum with  $65^{\circ}$  incidence angle. The reflectivity does not alter the pulse shape, while the phase shift does. The dotted line on the two uppermost figures has been added to increase the readability, and does not have the dimension indicated on the axis. The dashed lines in the other figures show the pulse shape before reflection.



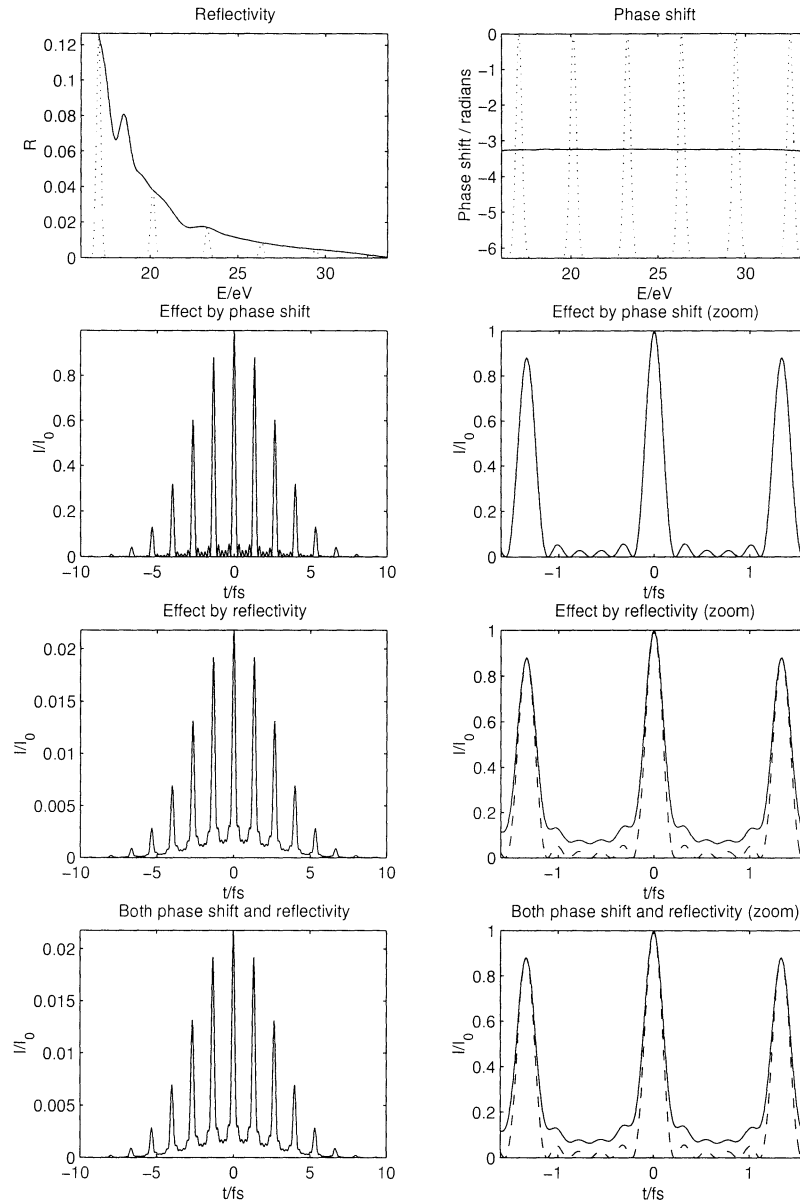


Figure 3.4: Pulse change at a reflection on aluminum with normal incidence. The phase shift does not alter the pulse shape, while the reflectivity does. The dotted line on the two uppermost figures has been added to increase the readability, and does not have the dimension indicated on the axis. The dashed lines in the other figures show the pulse shape before reflection. (To suppress the effect from the band edge, only 11th to 21st harmonic was used.)

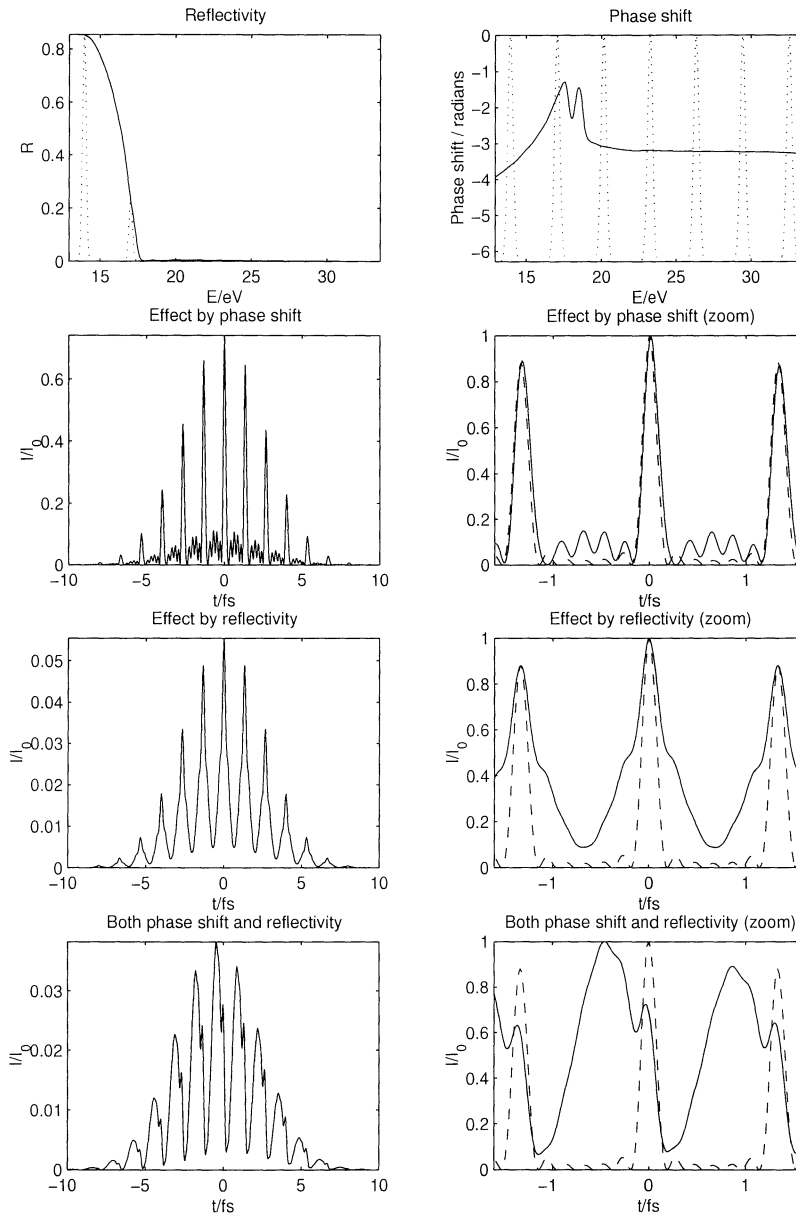


Figure 3.5: Pulse change at a reflection on aluminum with  $30^{\circ}$  incidence angle. Both the reflectivity and the phase shift alter the pulse shape. The dotted line on the two uppermost figures has been added to increase the readability, and does not have the dimension indicated on the axis. The dashed lines in the other figures show the pulse shape before reflection.

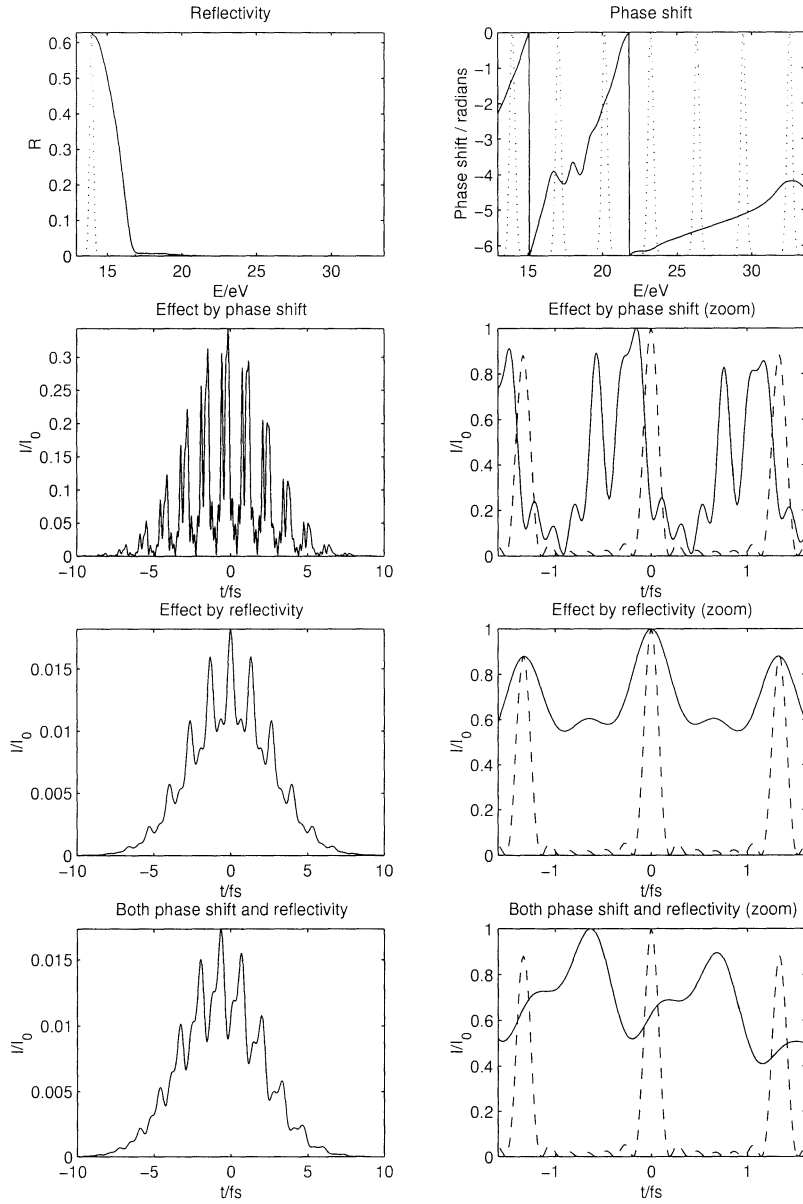


Figure 3.6: Pulse change at a delay line. The dotted line on the two upper-most figures has been added to increase the readability, and does not have the dimension indicated on the axis. The dashed lines in the other figures show the pulse shape before reflection.

## Chapter 4

# Reflection on curved surfaces

### 4.1 Introduction

Reflective optics often means curved mirrors. The main difference from plane mirrors is that the angle of incidence, and hence the phase shift, varies over the surface. An additional effect that stretches the pulse is the phase shift introduced by the aberrations.

### 4.2 Calculations

In order to demonstrate the magnitude of the effects, calculations were made for a specific case. The assumptions for those calculations are based on an experiment carried out in the department. In the experiment, the 5th harmonic was used, and it was focused using a spherical aluminum mirror with a focal length of 12 cm. The source was placed 3.0 m away from the mirror, which gave a focal spot 12.5 cm from the mirror. The fundamental beam from which the harmonics were generated was a femtosecond laser pulse at 800 nm. A Gaussian pulse shape was assumed, and the divergence was assumed to be 4 mrad, giving a spot size of 12 mm on the mirror. The size of the point where the harmonics were generated was neglected. Furthermore, cylindrical symmetry was assumed, and the resulting E-field was calculated as (see reference [11] section 16.2)

$$E_{res}(\lambda) = \int_0^R \frac{E_{in}(r, \lambda)}{d(r)} \exp(i \frac{2\pi}{\lambda} d(r)) r_{p/s}(\theta(r), \lambda) 2\pi r dr \quad (4.1)$$

where  $z = f(r)$  describes the mirror surface,

$$d(r) = \sqrt{(f(r) - d_{source})^2 + r^2} + \sqrt{(f(r) - d_{target})^2 + r^2} \quad (4.2)$$

is the distance from the source to the target, and

$$\theta(r) = \arccos \frac{f(r) - r \frac{df}{dr} - d_{source}}{\sqrt{\left(\left(\frac{df}{dr}\right)^2 + 1\right) \left(\left(r \frac{df}{dr}\right)^2 + (d_{source} - f(r))^2\right)}} \quad (4.3)$$

is the angle of incidence. The integral was approximated with a sum

$$E_{res}(\lambda) = \sum_{j=1}^N \frac{E_{in}(r_j, \lambda)}{d(r_j)} \exp(i \frac{2\pi}{\lambda} d(r_j)) r_{p/s}(\theta(r_j), \lambda) 2\pi r_j \Delta r \quad (4.4)$$

where  $r_j = jr_{max}/N$  and  $\Delta r = r_{max}/N$ . The MATLAB program used for the calculations can be found in Appendix A.

### 4.3 Results

Figure 4.1 shows how the pulse shape is altered by a reflection on an aluminum spherical mirror. Due to the low reflection for the higher order harmonics, the pulse is stretched in time. The almost linear phase shift gives the pulse an asymmetric “tail”.

Figure 4.2 and Figure 4.3 show how the pulse is altered by a reflection on gold and platinum, respectively. Since the reflectivity for the higher order harmonics of these mirrors are higher than for the aluminum mirror, the pulse is not stretched in the same way.

In the region of interest for attosecond optics, the reflectivity for on axis mirrors is very low. The intensity in the focal point is only 1,5% of the intensity in the source point for an aluminum mirror. The corresponding value for gold and platinum is 2.2% and 3.1%, respectively.

### 4.4 Conclusions

A normal incidence single layer spherical mirror is not usable as XUV optics in most cases. If it is used, precautions must be taken to minimize the effects from the aberration. The choice of material is also important, and depends on the wavelength range of interest.

In order to decrease the losses there are two possibilities. Either to use grazing incidence mirrors, or to use multilayer mirrors. However, both methods give rise to problems. Grazing incidence mirrors introduces aberrations, and

to minimize this, elliptical mirrors have to be used. Those mirrors can be very expensive.

The most simple multilayer mirrors are very narrow banded, and are not useful as attosecond optics. Today, there are broadband multilayer mirrors for femtosecond infrared laser pulses. The difference from normal broadband mirrors is that these mirrors do not introduce a chirp in the pulse, which means that there is no wavelength dependent phase shift. Maybe it would be possible to manufacture the same kind of mirrors for attosecond pulses, but there are several problems. For example, the layers would be absorbing the light, which would decrease the power. It would only be possible to use a few thin layers. Basic information about multilayer mirrors can be found in reference [10].

Due to a limited time, no calculations have been done on grazing incidence or multilayer mirrors. It would be interesting to examine this in the future.

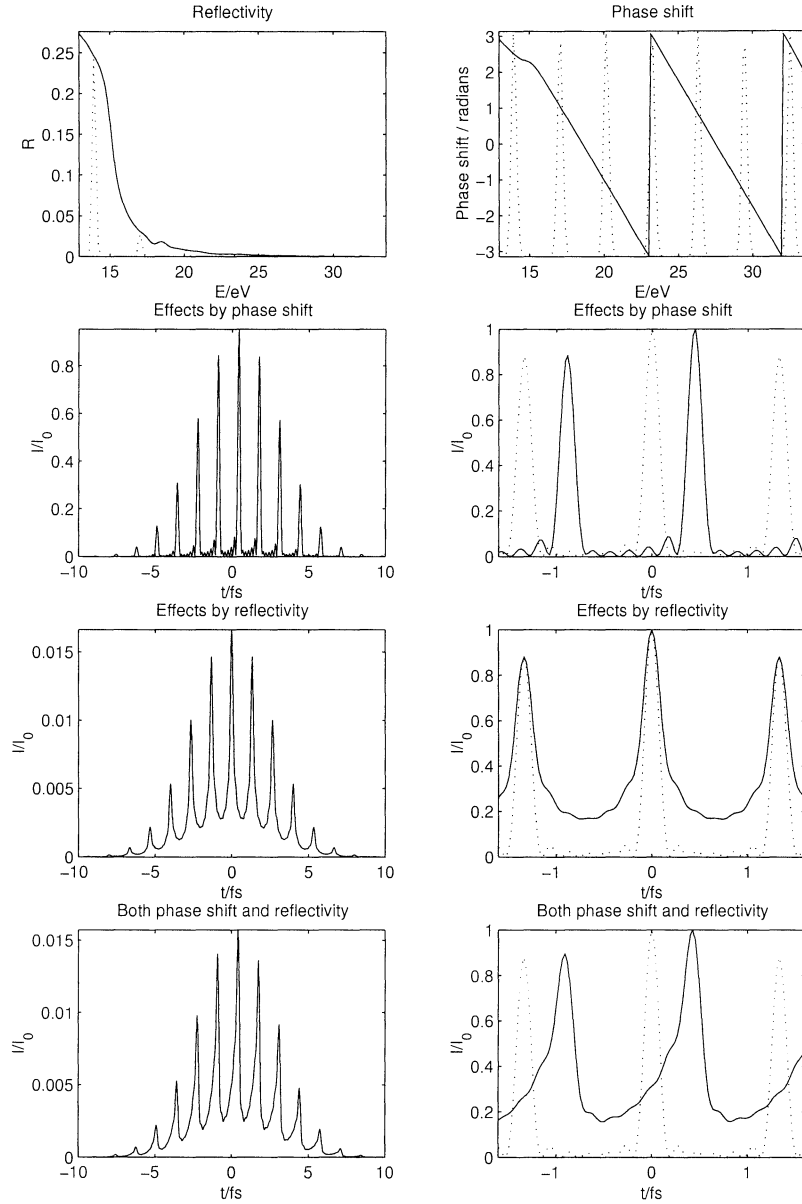


Figure 4.1: Attosecond pulses in the focus of an aluminum mirror. The dotted lines on the two uppermost figures have been added to increase the readability, and do not have the dimension indicated on the axis. The dotted lines in the other figures show the pulse shape before reflection.

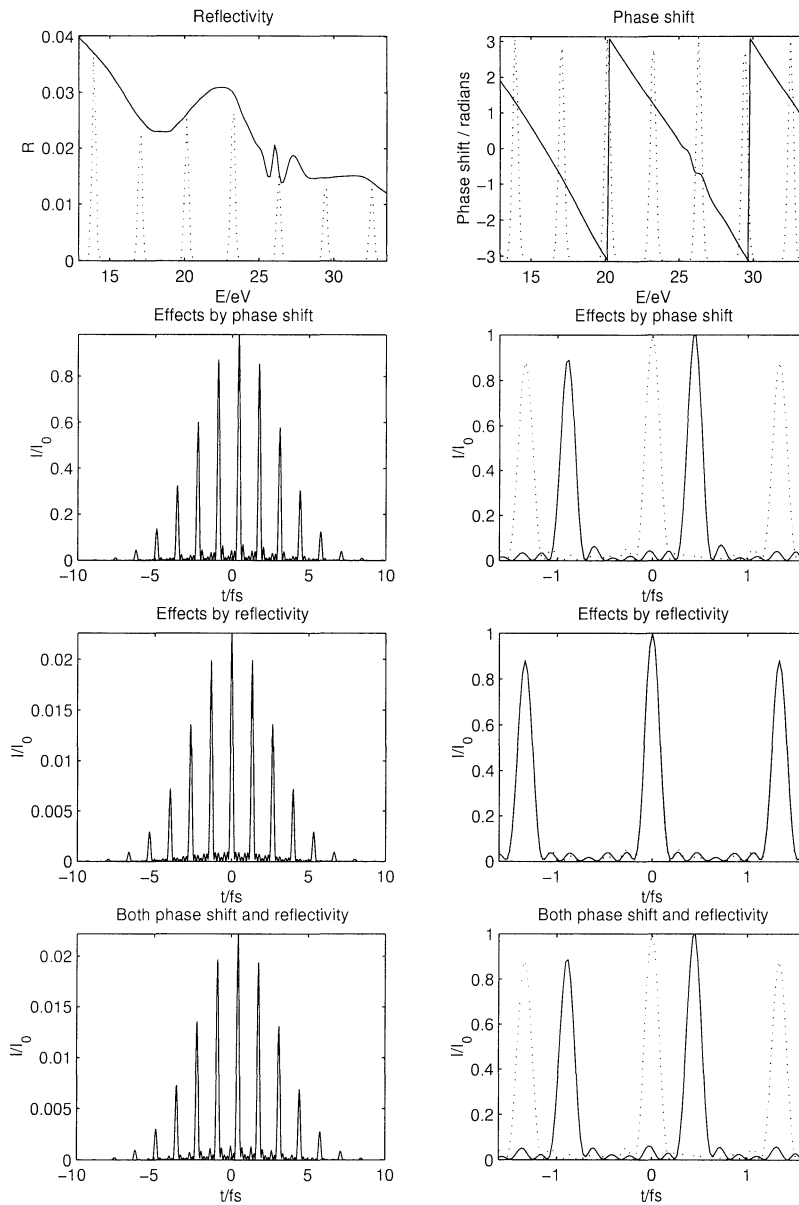


Figure 4.2: Attosecond pulses in the focus of a gold mirror. The dotted lines on the two uppermost figures have been added to increase the readability, and do not have the dimension indicated on the axis. The dotted lines in the other figures show the pulse shape before reflection.



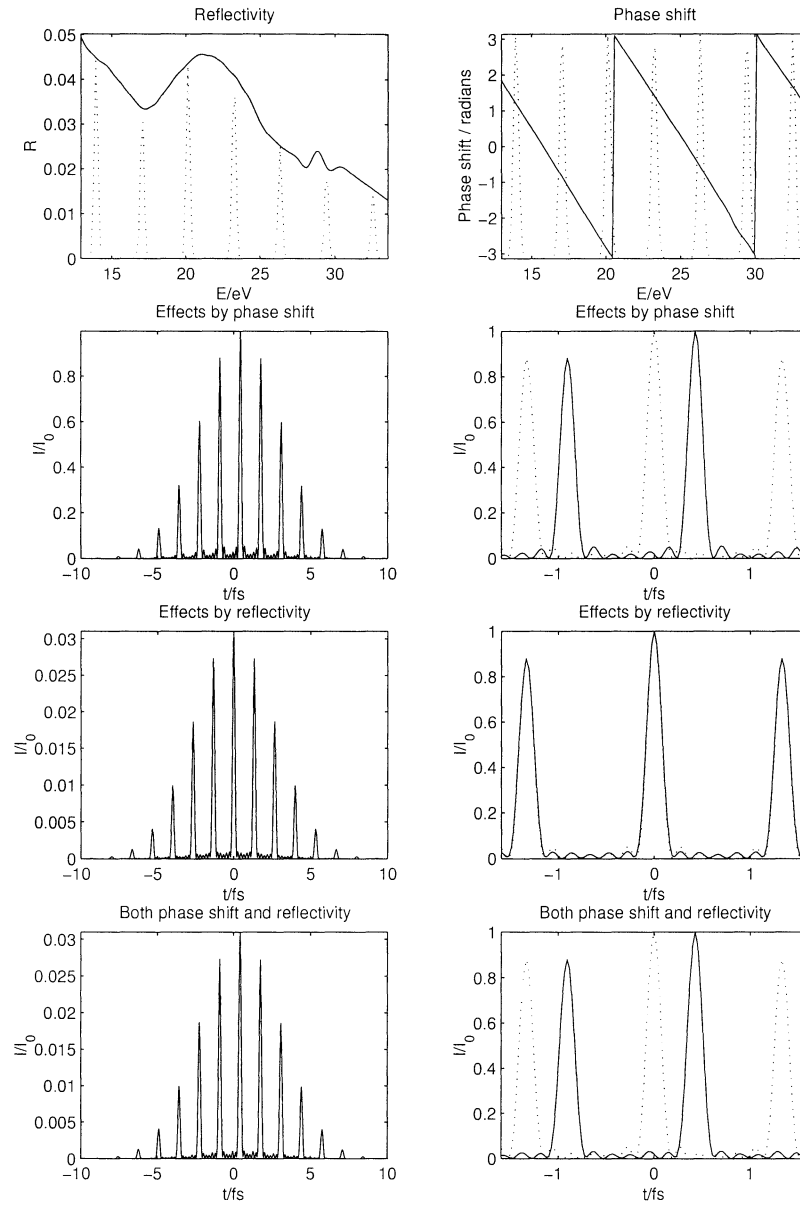


Figure 4.3: Attosecond pulses in the focus of a platinum mirror. The dotted lines on the two uppermost figures have been added to increase the readability, and do not have the dimension indicated on the axis. The dotted lines in the other figures show the pulse shape before reflection.

## Chapter 5

# Diffractive XUV optics

### 5.1 Introduction

Diffractive optics means optics that uses diffraction to focus the beam. The Fresnel zone plate is the most well known kind of diffractive optics. Other kind of diffractive optics is gratings and crystals. The Fresnel zone plate works almost as a lens. Instead of making all optical path lengths equal, it makes all possible paths from the source to the focal point to differ by an integer number of wavelengths. The other paths are blocked. The phase shift is proportional to the distance divided by the wavelength. This gives the zone plate a large chromatic aberration.

### 5.2 Calculations

The resulting electric field was calculated as (see reference [11] section 16.2)

$$E_{res}(\lambda) = \int_0^R E_{in}(\lambda, r) \frac{\exp(i2\pi d(r)/\lambda)}{d(r)} t(r) dr \quad (5.1)$$

where  $t(r) = 1$  if  $|d(r)/\lambda - \lfloor d(r)/\lambda \rfloor| < \pi/2$ , 0 otherwise, and  $d(r)$  is the path length from the source to the focal point. Again, the integral was approximated with a sum

$$E_{res}(\lambda) = \sum_{j=0}^N E_{in}(\lambda, r_j) \frac{\exp(i2\pi d(r_j)/\lambda)}{d(r_j)} t(r_j) \Delta r \quad (5.2)$$

where  $r_j = jr_{max}/N$  and  $\Delta r = r_{max}/N$ .

### 5.3 Results

Figure 5.1 shows the stretching of the 5th harmonic. The stretch depends on the number of zones on the zone plate. In this case it was 39. The reason for the stretch is that the light transmitted through the outer parts of the zone plate travels a longer distance than the light transmitted through the center.

The effect can also be described in the frequency domain. The zone plate works as a circular grating. The more zones a zone plate has, the more selective it is. The zone plate only focuses the central part of the broad spectrum of the femtosecond pulse onto the focal spot. Since the pulse becomes more narrowbanded, it also becomes longer in time.

This effect can also be seen in Figure 5.2. In the upper figure, where the zone plate is made for the 15th harmonic, the pulse is longer than the entire attosecond pulse train. If the entire 15th harmonic were selected, the pulse would have been no longer than the pulse train.

As mentioned earlier, all the beams have the same optical path length from the source to the focal point. This is, however, true for more than one point. There are several orders of focal points (as there are several orders for gratings). The first order is the one that is most far from the zone plate, and where most of the energy of the pulse arrives. The higher order focal points are closer to the zone plate, and less energy arrives here.

If a zone plate is manufactured for the fundamental wavelength, each harmonic will have a higher order focal point at the first order focal point of the fundamental beam. This can easily be realized by thinking in terms of interference. The harmonics have an integer number of wavelengths on one wavelength of the fundamental beam. Thus, if the interference from the fundamental beam is constructive, the interference for each harmonic will be constructive.

The lower part of Figure 5.2 shows the result when a zone plate made for the fundamental is used. Since there is less power in the higher order focal points, this gives rise to a great loss of energy. The peak power is only one fourth of the peak power when a zone plate for the 15th harmonic is used, and the total pulse energy is much less.

Even if the zone plate in this case has one transmission peak for each harmonic, each peak is narrower than the harmonic. This makes the attosecond pulse train longer, while the attosecond pulses are almost as short as before.

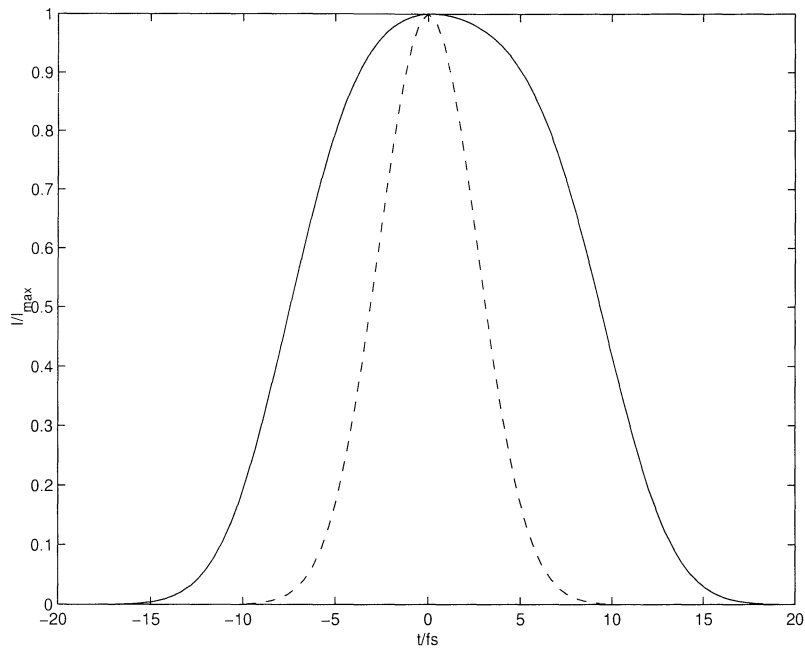


Figure 5.1: Stretching of the 5th harmonic by a zone plate with 39 zones. The dashed line shows the original pulse.

## 5.4 Conclusions

Zone plates can be used to focus single a harmonic. If the pulse is very short from the beginning, it will be stretched. However, in some cases this may be acceptable.

For use with attosecond pulses, zone plates are more or less useless. If a zone plate for the fundamental is used, the loss of energy will be much larger than acceptable in most situations. If a zone plate for a harmonic is used, it will filter out that specific harmonic, leaving a femtosecond pulse instead of an attosecond pulse train.

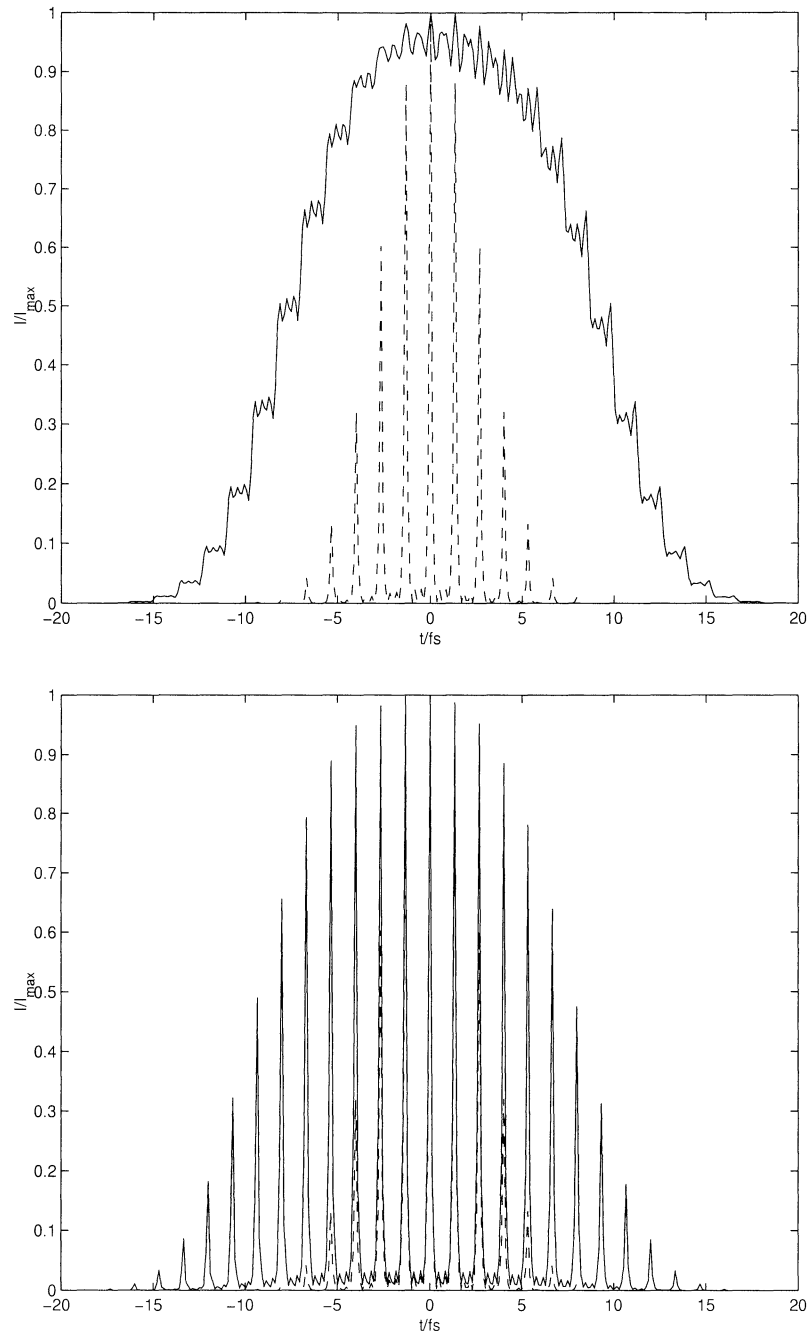


Figure 5.2: Stretching of an attosecond pulse train by a zone plate. The upper figure shows the stretching by a zone plate made for the median harmonic, and the lower the stretching by a zone plate made for the fundamental. The dashed line shows the original pulse.

## Chapter 6

# Conclusions and perspectives

The calculations done show that mirrors are better than zone plates in most cases. Zone plates can be used when the objective is to select and focus one out of many harmonics in a beam.

Spherical mirrors can be used without leaving any significant stretching of the pulse, but the reflectivity is generally very low, and other ways of focusing the attosecond pulses must be found.

I believe that the two most promising methods are grazing incidence elliptical mirrors and multilayer mirrors. There are many questions about this that need to be answered. Is it possible to manufacture elliptical mirrors with low aberrations at a reasonable cost? Is it possible to make multilayer mirrors with a broad reflection peak and a phase shift not dependent on the wavelength?

The next thing to do in this project would have been to do calculations on elliptical mirrors. To be able to do these calculations, cylindrical symmetry cannot be assumed. Hence, more computational power would be needed. The results would probably be very interesting.

Furthermore, calculations on multilayer mirrors could be done. It requires a lot of work to implement this, but it could generate some interesting results. Knowledge from multilayer mirrors for femtosecond pulses could be used to design a broadband mirror for attosecond pulses.

# Acknowledgement

First, I would like to thank my supervisors Anne L'Huilier and Claes-Göran Wahlström for all their help with this project. They have provided me with useful information, as well as inspiration.

I would also like to thank all the PhD-students and post docs on the department that have helped me in one or another way.

A special thank goes to Ida Karlsson for reading the report and giving very good suggestions on how the report could be made more readable.

# Bibliography

- [1] J D Kmetec, J J Macklin and J F Young, “0.5-TW, 125-fs Ti:sapphire laser”, *Optics Letters*, vol. 16, no. 13, pp. 1001-1003, July 1991.
- [2] C-G Wahlström, J Larsson, A Persson, T Starczewski, S Svanberg, P Salières, P Balcou and A L’Huillier, “High-order harmonic generation in rare gases with an intense short-pulse laser”, *Physical Review A*, vol. 48, no. 6, pp. 4709-4720, December 1993.
- [3] A L’Huillier, K J Schafer, K C Kulander, “Theoretical aspects of intense field harmonic generation”, *Journal of Physics B*, vol. 24, no. 15, pp. 3315-3341, 1991
- [4] H S Nguyen, A Suda, K Midorikawa, “Generation and propagation of attosecond pulses in He gas with sub-10-fs driver pulses”, *Physical Review A*, vol. 60, no. 3, pp. 2587-2590, 1999
- [5] N M Ceglio, “Revolution in X-Ray Optics”, *Journal of X-Ray Science and Technology*, vol. 1, no. 1, pp. 18-20, July 1989.
- [6] E Hecht, “Optics”, 3rd edition, Addison-Wesley 1998.
- [7] A G Michette, C J Buckley, “X-ray science and technology”, pp. 254-259, Bristol Institute of Physics Publishing cop. 1993
- [8] S-G Pettersson, S Borgström and H Hertz, “Advanced Optics”, KFS i Lund AB 1999.
- [9] E D Palik, “Handbook of optical constants of solids”, Academic Press Inc. 1985
- [10] <http://www-cxro.lbl.gov/>, Center for X-Ray Optics, Lawrence Berkeley National Laboratory.
- [11] A E Siegman, “Lasers”, University Science Books 1986



# Appendix A

## Program listings

### A.1 Reflection coefficients

```
function r=rp(vi, ni, nt)

vt=asin(ni./nt.*sin(vi));
r=(nt.*cos(vi) - ni.*cos(vt))./(ni.*cos(vt) + nt.*cos(vi));
```

```
function r=rs(vi, ni, nt)

vt=asin(ni./nt.*sin(vi));
r=(ni.*cos(vi)-nt.*cos(vt))./(ni.*cos(vi)+nt.*cos(vt));
```

### A.2 3D plot reflectivity and phase shift

The following program plots the reflectivity and phase shift for p-polarization. By changing rp to rs, the reflectivity and phase shift for s-polarization is calculated.

```
function reflect(mat, E1, E2)

if nargin < 1
    mat='A1';
end
if nargin < 3
    E1=10;
end
if nargin < 4
    E2=30;
end

% Constants
h=4.1357e-15;    % eVs
hbar=h/(2*pi);
```

```

c=299792458;
N=2^14;

% Create angle and energy scale
e=E1:(E2-E1)/90:E2;
v=0:90;
[E,V]=meshgrid(e,v);

% Reflection
load(['index/' mat])
eval(['n=spline(' mat '(:,1), ' mat '(:,2), E);']);
r_p=rp(rad(V), 1, n);
R=abs(r_p).^2;
P=angle(r_p);
t=find(P>0);
P(t)=P(t)-2*pi;

% Plots
figure(1)
mesh(E, V, P)
xlabel('Photon energy / eV')
ylabel('Angle of incidence / degrees')
zlabel('Phase shift / radians')
view([-1 -0.5 1])
a=axis;
a(4)=90;
axis(a)

figure(2)
mesh(E, V, R)
xlabel('Photon energy / eV')
ylabel('Angle of incidence / degrees')
zlabel('Reflectivity')
view([1 -1 1])
a=axis;
a(4)=90;
axis(a)

```

### A.3 Reflection on plane surface

This program calculates how a pulse is changed when it is reflected on a surface, and presents the information in an informative way.

```

function pulse(mat, v, n1, n2, dt, 10)

if nargin < 1
    mat='Al';
end
if nargin < 2
    v=45;
end
if nargin < 3
    n1=09;
end
if nargin < 4
    n2=21;
end
end

```

```

if nargin < 5
    dt=10e-15;
end
if nargin < 6
    l0=800e-9;
end

% Constants
h=4.1357e-15; % eVs
hbar=h/(2*pi);
c=299794258;
N=2^14;

% Fundamental pulse
dE=h/dt;
E0=h*c/l0;
dT=h/E0;

% Create time and energy scale
DE=200*E0/N;
DT=h/(N*DE);
E=(0:N-1)*DE;
t=(-N/2:N/2-1)*DT;

% Create pulse spectra
I=zeros(size(E));
for i=n1:2:n2
    I=I+gauss(E, i*E0, dE);
    %I=I+gauss(i, (n1+n2)/2, n2-n1)*gauss(E, i*E0, dE);
end

% Pulse before reflection
E1=ifft(I);
E1=[E1(N/2+1:N) E1(1:N/2)];
I1=E1.*conj(E1);

% Reflection
load(['index/' mat])
eval(['n=spline(' mat '(:,1), ' mat '(:,2), E);']);
r_p=rp(rad(v), 1, n);
r_refl=abs(r_p);
r_phase=r_p./r_refl;
Ip = I.*r_p;
Iphase = I.*r_phase;
Irefl = I.*r_refl;
R=abs(r_p).^2;
P=angle(r_p);
b=find(P>0);
P(b)=P(b)-2*pi;

% Pulse after reflection
E2=ifft(Ip);
E2=[E2(N/2+1:N) E2(1:N/2)];
I2=E2.*conj(E2);

E3=ifft(Iphase);
E3=[E3(N/2+1:N) E3(1:N/2)];
I3=E3.*conj(E3);

E4=ifft(Irefl);
E4=[E4(N/2+1:N) E4(1:N/2)];
I4=E4.*conj(E4);

```

```

% Plots
figure(1)

subplot(421)
plot(E, R, E, abs(Ip).^2, ':')
axis([E0*n1-1 E0*n2+1 0 max(R(floor(n1*E0/DE):floor(n2*E0/DE)))]])
title('Reflectivity')
xlabel('E/eV')
ylabel('R')

subplot(422)
plot(E, P, E, (I-1)*2*pi, ':')
axis([E0*n1-1 E0*n2+1 -2*pi 0 ])
title('Phase shift')
xlabel('E/eV')
ylabel('Phase shift / radians')

subplot(423)
plot(t, I3/max(I1))
axis([-dt dt 0 max(I3)/max(I1)])
title('Effects by phase shift')
xlabel('t/s')
ylabel('I/I_0')

subplot(424)
plot(t, I3/max(I3), '- ', t, I1/max(I1), ':')
axis([-dT*0.6 dT*0.6 0 1])
title('Effects by phase shift')
xlabel('t/s')
ylabel('I/I_0')

subplot(425)
plot(t, I4/max(I1))
axis([-dt dt 0 max(I4)/max(I1)])
title('Effects by reflectivity')
xlabel('t/s')
ylabel('I/I_0')

subplot(426)
plot(t, I4/max(I4), '- ', t, I1/max(I1), ':')
axis([-dT*0.6 dT*0.6 0 1])
title('Effects by reflectivity')
xlabel('t/s')
ylabel('I/I_0')

subplot(427)
plot(t, I2/max(I1))
axis([-dt dt 0 max(I2)/max(I1)])
title('Both phase shift and reflectivity')
xlabel('t/s')
ylabel('I/I_0')

subplot(428)
plot(t, I2/max(I2), '- ', t, I1/max(I1), ':')
axis([-dT*0.6 dT*0.6 0 1])
title('Both phase shift and reflectivity')
xlabel('t/s')
ylabel('I/I_0')

```

## A.4 Reflection on curved surface

```
mat='P1';
n1=09;
n2=21;
dt=10e-15;
l0=800e-9;

unit=40e-6;
N=450;
source=3/unit;
f=0.12/unit;
%f=1.5/unit;
target=1/(1/f-1/source);
R=(1:N);
w=12e-3/unit;
mirror=2*f-sqrt((2*f).^2-R.^2);

% Constants
h=4.1357e-15; % eVs
hbar=h/(2*pi);
c=299794258;
N=2^10;

% Fundamental pulse
dE=h/dt;
E0=h*c/l0;
dT=h/E0;

% Create time and energy scale
DE=100*E0/N;
DT=h/(N*DE);
E=(1:N)*DE;
t=(-N/2:N/2-1)*DT;

% Create pulse spectra
I=zeros(size(E));
for a=n1:2:n2
    I=I+gauss(E, a*E0, dE);
end

% Pulse before reflection
E1=ifft(I);
E1=[E1(N/2+1:N) E1(1:N/2)];
I1=abs(E1).^2;

% Reflection
Ip=fmir(mat, source, target, mirror, unit, w, E, I);
R=(abs(Ip)./(abs(I))).^2;
P=angle(Ip);

% Pulse after reflection
E2=ifft(Ip);
E2=[E2(N/2+1:N) E2(1:N/2)];
I2=abs(E2).^2;

E4=ifft(abs(Ip));
E4=[E4(N/2+1:N) E4(1:N/2)];
I4=abs(E4).^2;

E3=ifft(I.*exp(i*angle(Ip)));
```

```

%E3=ifft(I.*Ip./abs(Ip));
E3=[E3(N/2+1:N) E3(1:N/2)];
I3=abs(E3).^2;

% Plots

subplot(421)
plot(E, R, E, abs(Ip).^2, ':')
axis([E0*n1-1 E0*n2+1 0 max(R(floor((n1*E0-1)/DE):floor((n2*E0+1)/DE))])
title('Reflectivity')
xlabel('E/eV')
ylabel('R')

subplot(422)
plot(E, P, E, (I-0.5)*2*pi, ':')
axis([E0*n1-1 E0*n2+1 -pi pi])
title('Phase shift')
xlabel('E/eV')
ylabel('Phase shift / radians')

subplot(423)
plot(t*1e15, I3/max(I1))
axis([-dt*1e15 dt*1e15 0 max(I3)/max(I1)])
title('Effects by phase shift')
xlabel('t/fs')
ylabel('I/I_0')

subplot(424)
plot(t*1e15, I3/max(I3), '- ', t*1e15, I1/max(I1), ':')
axis([-dT*0.6*1e15 dT*0.6*1e15 0 1])
title('Effects by phase shift')
xlabel('t/fs')
ylabel('I/I_0')

subplot(425)
plot(t*1e15, I4/max(I1))
axis([-dt*1e15 dt*1e15 0 max(I4)/max(I1)])
title('Effects by reflectivity')
xlabel('t/fs')
ylabel('I/I_0')

subplot(426)
plot(t*1e15, I4/max(I4), '- ', t*1e15, I1/max(I1), ':')
axis([-dT*0.6*1e15 dT*0.6*1e15 0 1])
title('Effects by reflectivity')
xlabel('t/fs')
ylabel('I/I_0')

subplot(427)
plot(t*1e15, I2/max(I1))
axis([-dt*1e15 dt*1e15 0 max(I2)/max(I1)])
title('Both phase shift and reflectivity')
xlabel('t/fs')
ylabel('I/I_0')

subplot(428)
plot(t*1e15, I2/max(I2), '- ', t*1e15, I1/max(I1), ':')
axis([-dT*0.6*1e15 dT*0.6*1e15 0 1])
title('Both phase shift and reflectivity')
xlabel('t/fs')
ylabel('I/I_0')

```

```

function Iout=fmir(mat, source, target, mirror, unit, w, Ein, Iin)

% All parameters are given in the same unit
%
% mat          the material that the mirror is made of
% source       distance from the mirror to the source
% target       distance from the mirror to the target
% mirror       distance from mirror plane to the mirror as function of r

% Constants
h=4.1357e-15;
hbar=h/(2*pi);
c=299792458/unit;

% Create grid
N=length(mirror);
[R,E]=ndgrid(1:N,Ein);

% Load index of refraction
load(['index/' mat]);
eval(['m=spline(' mat '(:,1), ' mat '(:,2), Ein);'])
n=zeros(size(R));
for a=1:N
    n(a,:)=m;
end

% Calculate reflectivity coefficients
mir=mirror(R);
dmir=mir;
dmir(2:N,,:)=diff(mir);
dmir(1,,:)=dmir(2,,:);
theta=pi-acos((mir+R.*dmir-source)./sqrt((dmir.^2+1).*((R.*dmir).^2+(source-mir).^2)));
r_p=rs(theta, 1, n);

% Initialize variables needed for the calculation
r=sqrt(R.^2+(mir-source).^2)+sqrt(R.^2+(mir-target).^2);

% Calculate the strength of the E-field at the target point
Iout=ones(N,1)*Iin;
Iout=Iout.*gauss(R, 0, w);
Iout=Iout./r.*exp(-i.*2.*pi.*r.*E./(h*c));
Iout=Iout.*2.*pi.*R;
Iout=Iout.*r_p;
Iout=sum(Iout);

```

## A.5 Focusing with zone plate

```

unit=2e-6;
source=-1/unit;
target=0.5/unit;
lambda0=800e-9/unit;
w=12e-3/unit;
M=2^09;
N=2^10;
R=(0:N-1);
lambda=lambda0/05;
l0=lambda0*unit;
dt=10e-15;

```

```

n1=05;
n2=05;

% Constants
h=4.1357e-15; % eVs
hbar=h/(2*pi);
c=299794258;

% Fundamental pulse
dE=h/dt;
E0=h*c/l0;
dT=h/E0;

% Create time and energy scale
DE=(n2+1)*E0/M;
DT=h/(M*DE);
E=(0:M-1)*DE;
t=(-M/2:M/2-1)*DT;

% Create pulse spectra
I=zeros(size(E));
for i=n1:2:n2
    I=I+gauss(E, i*E0, dE);
end

[transmission,mmax]=zoneplate(source, target, lambda, R);
%plot(transmission)

A=fdiff(source, target, transmission, unit, w, E, I);

E1=fftshift(iff(I));
I1=E1.*conj(E1);
E2=(iff(A));
[a,l]=max(abs(E2));
E2=E2([1:end 1:l-1]);
E2=fftshift(E2);
I2=E2.*conj(E2);

%subplot(221)
figure(1)
r=(abs(A)./abs(I)).^2;
rmax=max(r(floor(n1*E0/DE):floor(n2*E0/DE)));
plot(E, r)
axis([n1*E0-1 n2*E0+1 0 rmax])
%axis([n1*E0-1 n2*E0+1 0 1])
title('')
xlabel('E/eV')
ylabel('I_{out}/I_{in}')

%subplot(222)
%P=angle(A);
%plot(E, P)
%axis([n1*E0-1 n2*E0+1 -pi pi])
%title('Phase shift')
%xlabel('E/eV')
%ylabel('Phase shift/radians')

%subplot(212)
figure(2)
plot(t*1e15, I1/max(I1), '--', t*1e15, I2/max(I2))
axis([-2*dt*1e15 2*dt*1e15 0 1])
xlabel('t/fs')

```



```

ylabel('I/I_{max}')
max(I2)/max(I1)
mmax

%subplot(224)
%plot(R*unit, transmission)
%axis([0 max(R*unit) 0 1])
%title(sprintf('Number of zones: %i', mmax));
%xlabel('R/m')
%ylabel('T')

function Iout=fdiff(source, target, T, unit, w, Ein, Iin)

% All parameters are given in the same unit
%
% mat          the material that the mirror is made of
% source       distance from the mirror to the source
% target       distance from the mirror to the target
% mirror       distance from mirror plane to the mirror as function of r

% Constants
h=4.1357e-15;
hbar=h/(2*pi);
c=299792458/unit;

% Create grid
N=length(T);
[R,E]=ndgrid(1:N,Ein);

% Initialize variables needed for the calculation
r=sqrt(R.^2+source.^2)+sqrt(R.^2+target.^2)-source-target;

% Calculate the strength of the E-field at the target point
Iout=ones(N,1)*Iin;
Iout=Iout.*gauss(R, 0, w);
Iout=Iout./r.*exp(-i.*2.*pi.*r.*E./(h*c));
Iout=Iout.*2.*pi.*R;
Iout=Iout.*T(R);
Iout=sum(Iout);

```